# ASSESSMENT OF EMPIRICAL MODELS AND UNCERTAINTY AND SENSITIVITY STUDY OF A HIGH-VELOCITY STEAM CONDENSATION EXPERIMENT WITH TRACE

**W. Jaeger**
Karlsruhe Institute of Technology, Institute for Applied Thermofluidics
Kaiserstraße 12, 76131 Karlsruhe, Germany
wadim.jaeger@kit.edu

**W. Hering**
Karlsruhe Institute of Technology, Institute for Neutron Physics and Reactor Technology
Hermann-von-Helmholtz-Platz 1, 76344 Eggenstein-Leopoldshafen, Germany
wolfgang.hering@kit.edu

## ABSTRACT

High-velocity steam condensation experiments are recalculated using the best-estimate system code TRACE. TRACE is the thermal hydraulic reference code of the U.S. NRC for the simulation of LWRs, which requires a comprehensive and continuous validation process. Previous TRACE studies of these high-velocity steam condensation experiments show that some experimental cases can be reproduced in a very good manner, while some of them cannot be reproduced at all. Thereby, the standard TRACE code is used with the Kuhn, Schock and Peterson model for laminar flow and the Gnielinski model for turbulent flow. One of the questions imposed on the previous investigations is why some experimental scenarios can be reproduced, while others cannot, even though the applied input and boundary conditions indicate no extreme scenarios. The present investigation aims to identify the reason for these differences. Therefore, a twofold strategy is applied, where first an uncertainty and sensitivity study is performed with the standard empirical models and second the standard empirical model is replaced by others. The results show that some of the experimental scenarios cannot be reproduced with the alternative empirical models of Shah, Wilke and of Uehara and Kinoshita, too. With respect to the uncertainty and sensitivity study, it shows that the uncertainties have a quantitative influence on the results, but the qualitative behaviour is identical for all uncertainty cases. This study fosters the confidence of the standard empirical models for (high-velocity) steam condensation and shows that not all experimental scenarios can be reproduced with system codes at all.

**KEYWORDS**
Condensation, heat transfer, TRACE, uncertainty and sensitivity

## 1. INTRODUCTION TO HIGH-VELOCITY STEAM CONDENSATION

In this paper, simulation results for a high-velocity steam condensation experiment are presented. The simulations are performed with the best-estimate system code TRACE, as part of the ongoing validation effort within the CAMP agreement of the U.S. NRC. Thereby, the present investigation continues a previous investigation presented at the NURETH17 conference [1]. The reason for this continuation are the partially

satisfying simulation results. Simulations performed with the standard empirical model for steam condensation show that some of the experimental scenarios can be reproduced with high qualitative and quantitative agreement, see left plot of Figure 1. Though, some of the experimental scenarios elude, for unknown reasons, from a successful simulation. The comparison between experiment and simulation shows large discrepancies, see right plot Figure 1. Therefore, the main objective of this paper is to identify the reasons why the best-estimate system code TRACE is able to reproduce some experimental scenarios of a certain high-velocity steam condensation experiment, while it fails for others scenarios of the same experiment.

The subject of this study is an experiment carried out by Goodykoontz and Dorsch in 1967 [2]. In this experiment, a counter-current, single shell-and-tube heat exchanger is used to condensate high velocity steam, entering from top in the central copper pipe, while being cooled by water flowing upward in the annulus placed around the tube. A detailed description of the experiment and the input and boundary conditions are given in [2], while a summary is provided in section 3. As mentioned, for some cases, no agreement is given between measurement and calculation. A first evaluation did not reveal the reason for this behaviour. A possible explanation why different results are obtained for the experimental scenarios, is that the empirical model is not applicable at all and the "good" results are just lucky shots. Also, it could be possible that a, in principle, suitable empirical model is used with input and boundary conditions exceeding the validated parameter range for some scenarios. The user effect might cause the differences, if erroneous input and boundary conditions are entered into the input deck. The fourth reason might be related to erroneous measurements leading to wrong experimental data.

Based on the experience of the authors and the solid validation background of the TRACE system code, the option of using an inappropriate empirical model for steam condensation can be excluded. In addition, the experimental input and boundary conditions of the specific experimental scenarios are not out of bound. In fact, in several cases, the input and boundary conditions are in the central portion of the parameter range. The user effect can also be excluded, because the differences in the TRACE input for the different experimental scenarios are, basically, five parameters and their associate figures: Steam flow rate, temperature and pressure, and coolant flow rate and temperature. The input deck generation for the different experimental scenarios is automatized, based on tables with the five parameters. A careful double-check revealed that the correct numbers have been extracted from the original document and have been correctly entered into the input deck. With respect to the last cause, it is premature to draw the conclusion that the experiment is wrong from just one simulation by a single person. It would be reasonable if several simulations done with several empirical models and performed by several persons would deliver similar qualitative and quantitative results.

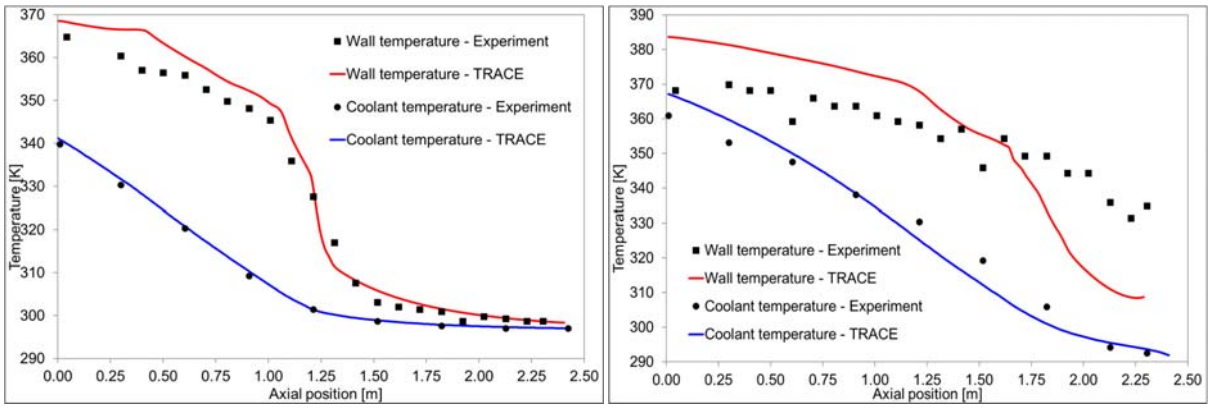


**Figure 1. Comparison of experimental (symbols) and calculated (lines) wall temperatures and coolant temperatures. Case 163 – left, case 175 – right. Labelling based on [2].**

To shed further light on the predicting options and capabilities, a twofold strategy is applied (see Figure 2). First, two representative cases, one with agreement (case 163) and one without agreement (case 175) between experiment and calculation, are selected for an uncertainty and sensitivity study (step 2 in Figure 2). The aim of this study is to evaluate if the variation of input and boundary conditions will cause perturbations, leading to a completely different qualitative and quantitative result. Second, the applicability of different empirical condensation models is assessed. Therefore, four different steam condensation models are programmed into the TRACE source code and the same two cases as for the uncertainty and sensitivity study are simulated (step 3 – 6 in Figure 2). For the present investigation, the simulations are limited to the two representative experimental scenarios only. Due to the computational burden of uncertainty and sensitivity studies, including around 100 simulations per experimental scenario, a complete simulation of all 58 different experimental scenarios would lead to roughly 5800 independent simulations, each lasting for several hours. This would exceed the timeframe of this investigation.

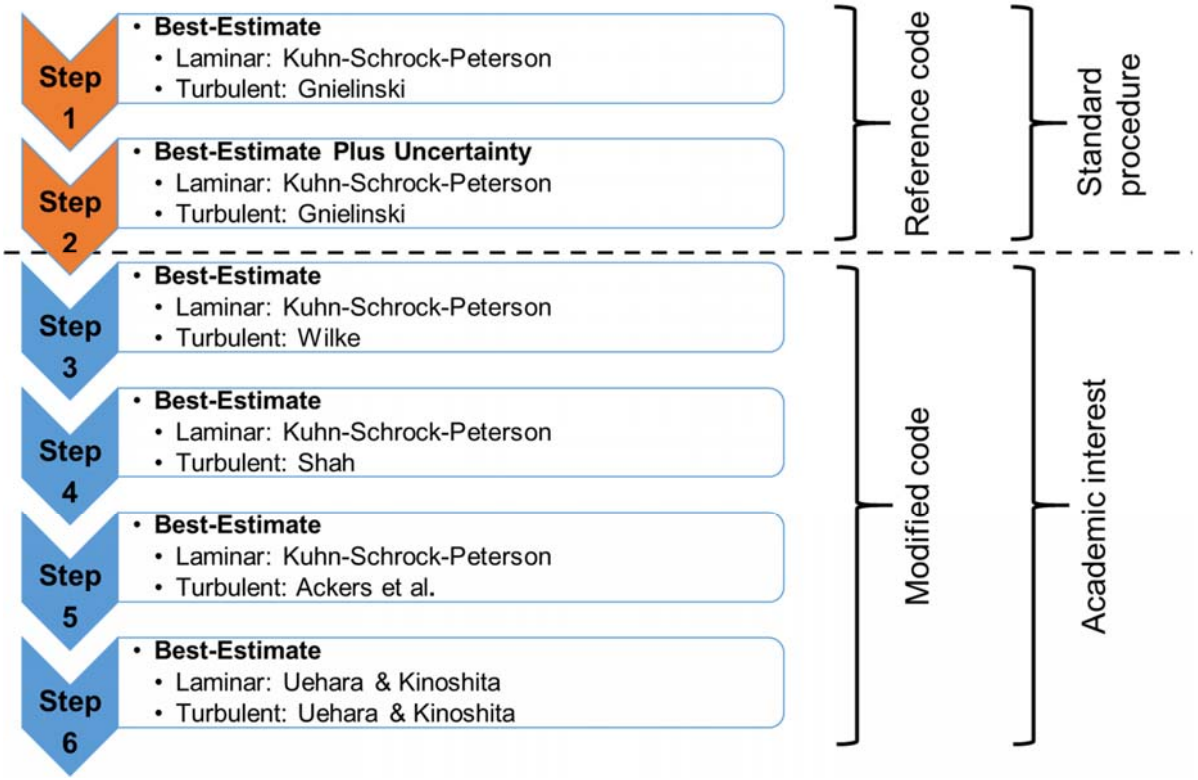


**Figure 2. Twofold simulation strategy for the high-velocity steam condensation experiment.**

## 2. FILM CONDENSATION HEAT TRANSFER MODELS

With respect to film condensation in nuclear power plant applications, two distinct modes of condensation can appear. The first one is falling film condensation, which is condensation on large surfaces like a containment wall. The second one is the sheared film condensation, which appears during high-velocity condensation in heat exchanger and condenser pipes. In order to cover both modes, the applied TRACE model must ensure its appropriateness over a large range of boundary conditions, determined by, e.g., the film Reynolds number. The main mode of condensation inside TRACE is the falling film condensation [3]. The definition of the film condensation within the TRACE system code reads as follows:

$$h = \mathrm{Nu}_{\mathrm{condensation}} \cdot \frac{k_{\mathrm{liquid}}}{\delta_{\mathrm{film}}}. \quad (1)$$

The characteristic length for the film condensation heat transfer ($h$) is thereby the liquid film thickness ($\delta_{\mathrm{film}}$), with $k$ being the thermal conductivity. To allow an application of a wide range of film Reynolds numbers, the film condensation model is based on laminar and turbulent flows. Therefore, a quadratic power law is established to weight the laminar and turbulent fraction on the heat transfer, see Eq. (2).

$$\mathrm{Nu}_{\mathrm{condensation}} = \sqrt{\left(\mathrm{Nu}_{\mathrm{laminar}}{}^{2} + \mathrm{Nu}_{\mathrm{turbulent}}{}^{2}\right)}. \quad (2)$$

With respect to the laminar heat transfer the Kuhn, Schrock and Peterson (KSP) [4][5] is used in TRACE. It is based on a comparison of the model with other models and an experimental database [3]. The original KSP model is used for the calculation of the Nusselt number across a film during condensation. To transfer this model into a model applicable for interfacial heat transfer, it is divided into two equal parts. One part is for the wall-to-liquid heat transfer and the other part is for the liquid-to-interface heat transfer. The final model, which has been implemented into TRACE by the TRACE developers reads now as follows:

$$\mathrm{Nu}_{\mathrm{laminar}} = 2 \cdot (1 + 1.83 \cdot 10^{-4} \cdot \mathrm{Re}_{\mathrm{film}}). \quad (3)$$

This model can be used for the wall heat transfer during laminar film condensation. The model for the turbulent heat transfer in TRACE is based on the model of Gnielinski [6]. This model usually applied to turbulent convective heat transfer in a pipe, is corrected to account for the film condensation. By assuming that the hydraulic diameter of a thin liquid film is simply four times the film thickness, a mean for the correction is found [3]. Thus, the Gnielinski model for film condensation reads as follows:

$$\mathrm{Nu}_{\mathrm{turbulent}}^{\mathrm{Gnielinski}} = \frac{1}{4} \cdot \frac{\frac{f}{2} \cdot (\mathrm{Re}_{\mathrm{film}} - 1000) \cdot \mathrm{Pr}_{\mathrm{film}}}{1 + 12.7 \cdot \sqrt{\frac{f}{2}} \cdot \left(\mathrm{Pr}_{\mathrm{film}}{}^{\frac{2}{5}} - 1\right)} \quad (4)$$

The factor f in the Gnielinski model is the friction factor according to Filonenko [7]

$$f = [1.58 \cdot \ln(\mathrm{Re}_{\mathrm{film}}) - 3.28]^{-2}. \quad (5)$$

The film Reynolds and film Prandtl number write as follows:

$$\mathrm{Re}_{\mathrm{film}} = \frac{G_{\mathrm{liquid}} \cdot d_{\mathrm{hydraulic}}}{\eta_{\mathrm{liquid}}}, \quad (6)$$

$$\mathrm{Pr}_{\mathrm{film}} = \frac{\eta_{\mathrm{liquid}} \cdot c_{p,\mathrm{liquid}}}{k_{\mathrm{liquid}}}. \quad (7)$$

Where $G$ is the mass velocity, $d$ is the diameter, $\eta$ is the dynamic viscosity, $c_p$ is the specific heat and $k$ is the thermal conductivity. The above presented models represent the models of the standard TRACE system code. Both, the laminar and turbulent heat transfer models are validated against experimental data and show a general applicability to a wide range of film Reynolds numbers. In the following, alternative models for the turbulent film condensation are introduced. These models are also based on validation with experiments. However, these models are rather complex and some of them require more than just the film Reynolds and film Prandtl number. The first alternative model selected is the one of Wilke [8].

$$\mathrm{Nu}_{\mathrm{turbulent}}^{\mathrm{Wilke}} = \begin{cases} \mathrm{MAX}\left[1.88, 2.93 \cdot 10^{-2} \cdot \mathrm{Re}_{\mathrm{film}}{}^{8/15} \cdot \mathrm{Pr}_{\mathrm{film}}{}^{0.344}\right] & : \quad \mathrm{Re}_{\mathrm{film}} < 1600 \\ 2.122 \cdot 10^{-4} \cdot \mathrm{Re}_{\mathrm{film}}{}^{6/5} \cdot \mathrm{Pr}_{\mathrm{film}}{}^{0.344} & : \quad 1600 < \mathrm{Re}_{\mathrm{film}} < 3200 \\ 1.81 \cdot 10^{-3} \cdot \mathrm{Re}_{\mathrm{film}}{}^{14/15} \cdot \mathrm{Pr}_{\mathrm{film}}{}^{0.344} & : \quad \mathrm{Re}_{\mathrm{film}} > 3200 \end{cases} \tag{8}$$

This model was also considered by the TRACE developers as standard model, but has not been selected, because of the wide range of applicability of the Gnielinski model and the fact that the Gnielinski model is also used for single-phase forced convection [3].

A second empirical model for condensation heat transfer is found in the Shah model [9, 10]. This model has been developed for steam, refrigerants and organic substances and should be used for mass velocities greater than 200 kg/m²s. With respect to the experimental scenarios, mass velocities of 70 to 250 kg/m²s are present, while the two selected case are in the range of 100 kg/m²s. The Shah model is a modification of the Dittus-Boelter correlation for single-phase forced convection

$$\mathrm{Nu}_{\mathrm{turbulent}}^{\mathrm{Shah}} = 0.023 \cdot \mathrm{Re}_{\mathrm{film}}{}^{0.8} \cdot \mathrm{Pr}_{\mathrm{film}}{}^{0.4} \cdot \left[ (1-x)^{0.8} + \frac{3.8 \cdot x^{0.76} \cdot (1-x)^{0.04}}{\left(\frac{p}{p_{\mathrm{critical}}}\right)^{0.38}} \right] \tag{9}$$

With $x$ being the vapour quality, $p$ being the local pressure and $p_{\mathrm{critical}}$ being the critical pressure. A model valid for smaller mass velocities is given by the Akers et al. model [11]. Like the previous model, this model is applicable to refrigerants and organics. Even though this model is originally developed for horizontal tubes, an application to the vertical tube cases in the present investigation is justifiable due to the small gravitational impact on the results. The Akers et al. model reads as follows:

$$\mathrm{Nu}_{\mathrm{turbulent}}^{\mathrm{Akers}} = \mathrm{C} \cdot \mathrm{Re}_{\mathrm{equil}}{}^{\mathrm{n}} \cdot \mathrm{Pr}_{\mathrm{film}}{}^{0.333} \tag{10}$$

With C = 0.0265 and n = 0.8 for $\mathrm{Re}_{\mathrm{equil}} > 50{,}000$, while C = 5.03 and n = 0.333 for $\mathrm{Re}_{\mathrm{equil}} \leq 50{,}000$. Akers et al. use an equilibrium Reynolds number instead of a film Reynolds number, which is defined as follows with $G$ as the mass velocity, $x$ as the vapour quality, $d$ is the diameter and $\rho$ as the density.

$$\mathrm{Re}_{\mathrm{equil}} = \frac{d_{\mathrm{hydraulic}}}{\eta_{\mathrm{liquid}}} \cdot G_{\mathrm{total}} \cdot \left[ (1-x) + x \cdot \left( \frac{\rho_{\mathrm{liquid}}}{\rho_{\mathrm{gas}}} \right)^{0.5} \right] \tag{11}$$

The last empirical model applied in this study is the model developed by Uehara and Kinoshita [12][13][14]. This model is derived from experiments on forced convection film condensation of refrigerants on a vertical surface. Thereby, this model covers the areas of laminar flow, sine wave flow, harmonic wave flow and turbulent flow. Because the Uehara and Kinoshita model consists of four parts, unlike the TRACE code (laminar and turbulent flow), Eq. (2) is not used. Instead, the condensation Nusselt number is calculated with the following piece-wise fashioned correlation matrix (UK = Uehara and Kinoshita):

$$\mathrm{Nu}_{\mathrm{laminar}}^{\mathrm{UK}} = 0.707 \cdot \left( \frac{\mathrm{Gr} \cdot \mathrm{Pr}_{\mathrm{film}}}{\mathrm{Ja}} \right)^{0.25} \tag{12}$$

$$\mathrm{Nu}_{\mathrm{sine\ wave}}^{\mathrm{UK}} = 1.65 \cdot \mathrm{So}^{-0.333} \cdot \left( \frac{\mathrm{Ja}}{\mathrm{Pr}_{\mathrm{film}}} \right)^{0.333} \cdot \left( \frac{\mathrm{Gr} \cdot \mathrm{Pr}_{\mathrm{film}}}{\mathrm{Ja}} \right)^{0.333} \tag{13}$$

$$\mathrm{Nu}^{\mathrm{UK}}_{\text{harmonic wave}} = 0.725 \cdot \left(\frac{\mathrm{Ja}}{\mathrm{Pr}_{\mathrm{film}}}\right)^{0.06667} \cdot \left(\frac{\mathrm{Gr} \cdot \mathrm{Pr}_{\mathrm{film}}}{\mathrm{Ja}}\right)^{0.2667} \tag{14}$$

$$\mathrm{Nu}^{\mathrm{UK}}_{\text{turbulent}} = 0.043 \cdot \mathrm{Ja}^{0.2} \cdot \mathrm{Gr}^{0.4} \tag{15}$$

The transition points from laminar to sine wave, from sine wave to harmonic wave and from harmonic wave to turbulent flow, respectively, are as follows:

$$\left(\frac{\mathrm{Gr} \cdot \mathrm{Pr}_{\mathrm{film}}}{\mathrm{Ja}}\right)_{\text{laminar}\rightarrow\text{sine wave}} = 3.83 \cdot 10^{-5} \cdot \mathrm{So}^{4} \cdot \left(\frac{\mathrm{Ja}}{\mathrm{Pr}_{\mathrm{film}}}\right)^{-4} \tag{16}$$

$$\left(\frac{\mathrm{Gr} \cdot \mathrm{Pr}_{\mathrm{film}}}{\mathrm{Ja}}\right)_{\text{sine wave}\rightarrow\text{harmonic wave}} = 4.39 \cdot 10^{-6} \cdot \mathrm{So}^{5} \cdot \left(\frac{\mathrm{Ja}}{\mathrm{Pr}_{\mathrm{film}}}\right)^{-4} \tag{17}$$

$$\left(\frac{\mathrm{Gr} \cdot \mathrm{Pr}_{\mathrm{film}}}{\mathrm{Ja}}\right)_{\text{harmonic wave}\rightarrow\text{turbulent}} = 1.39 \cdot 10^{9} \cdot \mathrm{Ja}^{-4} \cdot {\mathrm{Pr}_{\mathrm{film}}}^{2.5} \tag{18}$$

With Gr being the Grashof number, Ja the Jakob number and So the Soflata number, which are defined as follows:

$$\mathrm{Gr} = \left(\frac{g \cdot {\delta_{\mathrm{film}}}^{3}}{{\nu_{\mathrm{film}}}^{2}}\right) \cdot \left(\frac{\rho_{\mathrm{film}} - \rho_{\mathrm{gas}}}{\rho_{\mathrm{film}}}\right) \tag{19}$$

$$\mathrm{Ja} = \frac{c_{p,\mathrm{film}} \cdot \left(T_{\mathrm{gas}} - T_{\mathrm{wall}}\right)}{\Delta h_{\mathrm{vaporization}}} \tag{20}$$

$$\mathrm{So} = \left(\frac{3 \cdot \sigma}{{\rho_{\mathrm{film}}}^{3} \cdot g \cdot {\nu_{\mathrm{film}}}^{3}}\right)^{0.2} \tag{21}$$

Where $g$ is the acceleration of gravity, $\delta$ the film thickness, $\sigma$ surface tension, $\nu$ the kinematic viscosity, $\rho$ the density, $c_p$ the specific heat, $T$ the temperature, $\Delta h_{\mathrm{vaporization}}$ the heat of vaporization.

## 3. HIGH-VELOCITY STEAM CONDENSATION EXPERIMENT

In 1967 Goodykoontz and Dorsch published a report [2] dealing with high-velocity steam condensation. The experiments were performed at the Lewis Research Center, a NASA facility. The aim of this experiment is to demonstrate the feasibility of a Rankine-process to be used as a power system for space operation. By choosing high velocities, the corresponding Froude number of the condensation process becomes very large and is therefore comparable to a zero-gravity environment.

The rather simple design (one central tube surrounded by a second tube) makes it easily accessible for investigations with best-estimate system codes like TRACE. A sketch of the facility is given in Figure 3, while the actual test section is depicted on the left side of Figure 4. For the present investigation, only the test section (test condenser in Figure 3) is modelled with TRACE. The complete TRACE model consists of seven components: two PIPE components for the inner tube and the outer tube, two FILL components for each PIPE, serving as mass flow rate and initial temperature boundary conditions, two BREAK components for each PIPE, serving as pressure boundary condition and one HTSTR component to model the wall between inner and outer PIPE components. The TRACE model is depicted on the right side of Figure 4

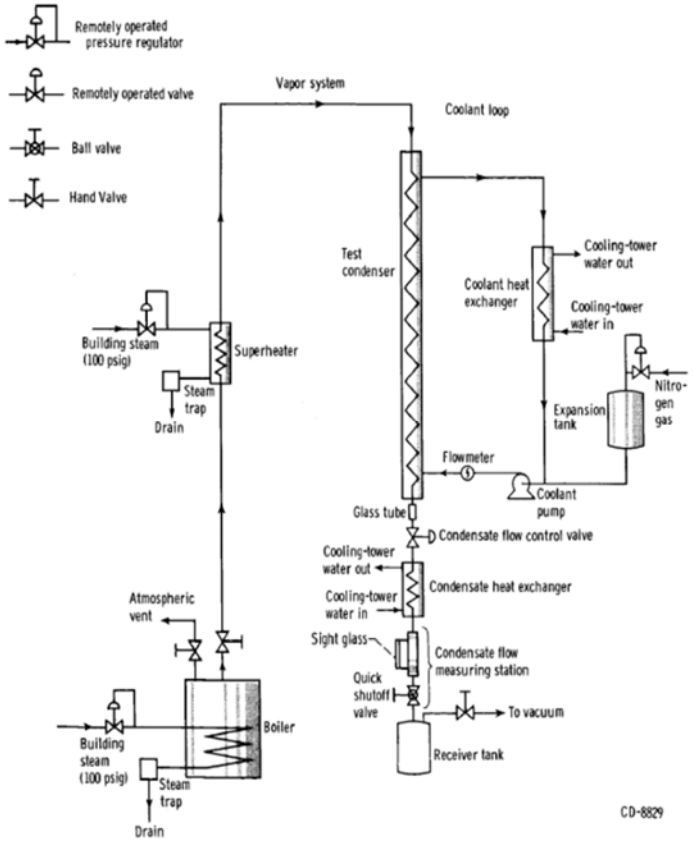


**Figure 3. Schematics of the fest facility for high-velocity steam condensation experiments [1][2].**

The high-velocity steam enters the inner PIPE component at the top (labelled 0.0 m in the plots to follow), while the coolant water enters the outer PIPE component at the bottom (labelled 2.4 m in the plots to follow). Thus, the two PIPE components create a counter-current, shell-and-tube heat exchanger. The two PIPE components are nodalized into 240 equidistant cells. Hence, each cell has a length of 10 mm. Such a fine nodalization is chosen to carefully evaluate, e.g., the location of full condensation, the development of the sensitivity coefficents over the length. The author is aware that such a refined geometry may not be suitable for system code applications, but with respect to empirical model assessment it might be of advantage rather than a coarse nodalization. That could mean that spatial information is either lost or blurred. The dimensions of the PIPE components (inner and outer diameters) are given in the left sketch of Figure 3. The main operational parameters of the experimental campaigns are summarized in Table I.

## 4. UNCERTAINTY AND SENSITIVITY STUDY

The uncertainty and sensitivity study is performed by applying the GRS method with the SUSA code system [15] [16]. SUSA follows the input error propagation, Wilks formula [17] and Monte Carlo sampling methods [18]. For each experimental scenario a list of uncertainty parameters including the range of uncertainty must be compiled. With Wilks formula, the number of calculations can be estimated in order to fulfil a certain statistical fidelity. For a confidence level of 95 % and a probability content of 95 % 93 simulations are necessary for the two-sided tolerance limit [18]. Then, Monte Carlo sampling methods are used to generate a specified number of values for each uncertain parameter. To assess the variations sensitivity of the uncertain parameters selected statistical measures, like the Pearson's product momentum coefficient [18], are calculated.

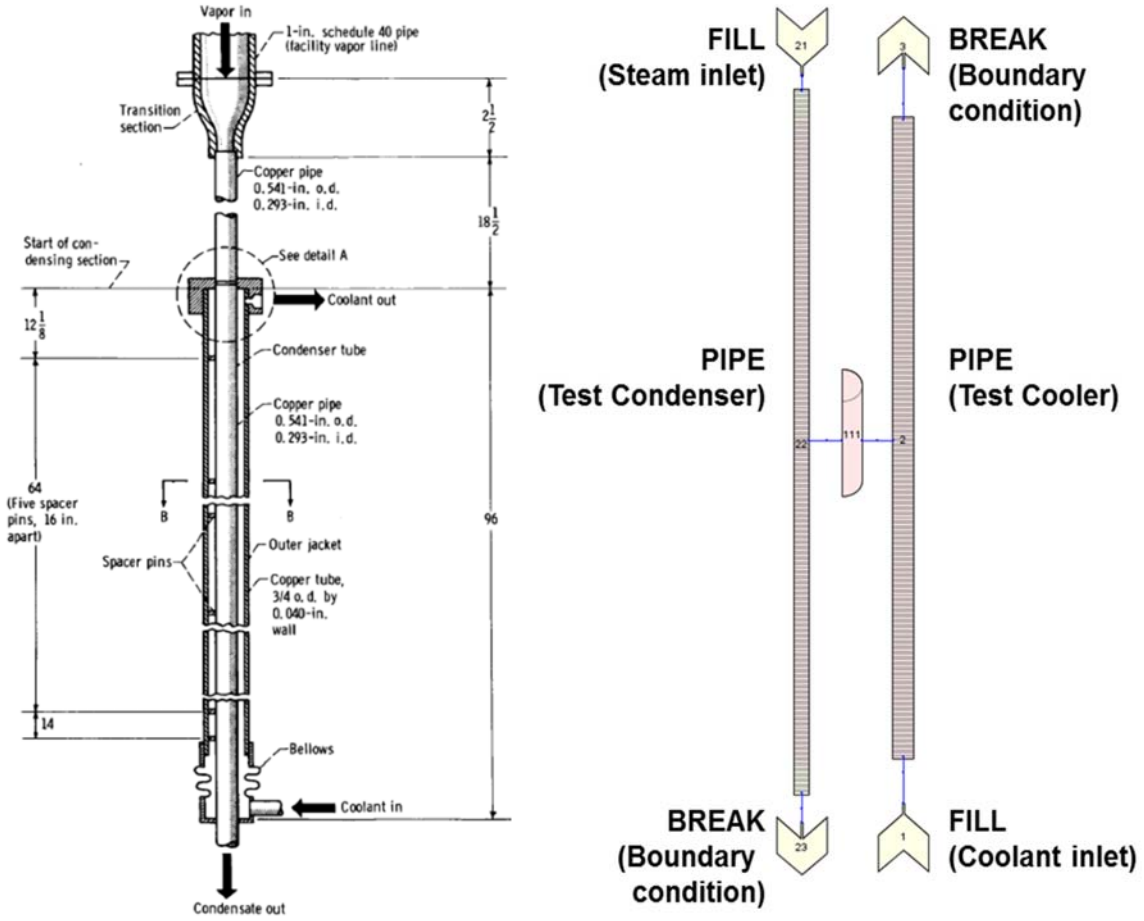


**Figure 4. Schematics of the test section (left) and TRACE model (right) for high-velocity steam condensation experiment**

**Table I. Operational conditions for the high-velocity steam condensation experiment [1][2].**

| **Parameters [Unit]** | **Parameter range** |
|---|---|
| Steam flow rate [kg/s] | 0.0038 … 0.0199 |
| Steam inlet pressure [bar] | 1.03 … 2.70 |
| Steam inlet temperature [K] | 386 … 417 |
| Steam inlet velocity [m/s] | 95 … 310 |
| Steam inlet quality [%] | > 99 |
| Condensing length [m] | 0.33 … 2.04 |
| Coolant flow rate [kg/s] | 0.0510 … 0.2747 |
| Coolant inlet temperature [K] | 289 … 310 |
| Coolant outlet temperature [K] | 308 … 370 |

For the present uncertainty and sensitivity study the following nine parameters are listed in Table II: Steam mass flow rate (kg/s, Par. 1), coolant mass flow rate (kg/s, Par. 2), steam temperature (K, Par. 3), coolant temperature (K, Par. 4), pressure in the condenser tube (Pa, Par. 5) and wall roughness (m, Par. 6).

Furthermore, multiplication factors for thermo-physical properties of the copper pipe are defined for the density (Par. 7), the thermal conductivity (Par. 8) and the specific heat (Par. 9. As mentioned above, the intention is to find out if changes of input parameters will provoke perturbations in output parameters. Furthermore, the measurement uncertainties from the experiment are not reported. Therefore, the parameter variation range is more based on maximal possible variations than on actual measured uncertainties.

The results of the uncertainty and sensitivity study is shown in Figure 5. The left plot shows the wall temperatures for case 163, while the right plot shows the wall temperatures for case 175. The main conclusion, which can be drawn from the graphs in Figure 5, is that the variations of the initial input and boundary conditions cause quantitative changes of the wall temperature. The qualitative trend is maintained and no perturbations have been introduced. Even the combination of extreme cases (such as a much higher inlet velocity paired with a much smaller inlet temperature and reduced heat transfer capabilities through the wall) did not provoke a substantial change in the wall temperature. This means, that the reason for the large discrepancies between experiment and calculation for experimental case 175 (and probably for the other unsatisfactory cases) cannot be explained with an empirical model being out of its application range.

**Table II. Uncertain parameters for experimental scenario 165 and 175.**

| | Run 165 | | | Run 175 | | |
|---|---|---|---|---|---|---|
| | **Reference** | **Minimum** | **Maximum** | **Reference** | **Minimum** | **Maximum** |
| **Par. 1** | 7.5599E-03 | 7.1819E-03 | 7.9379E-03 | 6.1487E-03 | 5.8413E-03 | 6.4561E-03 |
| **Par. 2** | 1.0458E-01 | 9.9349E-02 | 1.0981E-01 | 0.05102919 | 4.8478E-02 | 5.3581E-02 |
| **Par. 3** | 390.93 | 388.93 | 392.93 | 389.82 | 387.82 | 391.82 |
| **Par. 4** | 297.04 | 295.04 | 299.04 | 291.48 | 289.48 | 293.48 |
| **Par. 5** | 1.1680E+05 | 1.1096E+05 | 1.2264E+05 | 1.2955E+05 | 1.2307E+05 | 1.3603E+05 |
| **Par. 6** | 2.00E-05 | 1.00E-06 | 5.00E-05 | 2.00E-05 | 1.00E-06 | 5.00E-05 |
| **Par. 7** | 1 | 0.95 | 1.05 | 1 | 0.95 | 1.05 |
| **Par. 8** | 1 | 0.95 | 1.05 | 1 | 0.95 | 1.05 |
| **Par. 9** | 1 | 0.95 | 1.05 | 1 | 0.95 | 1.05 |

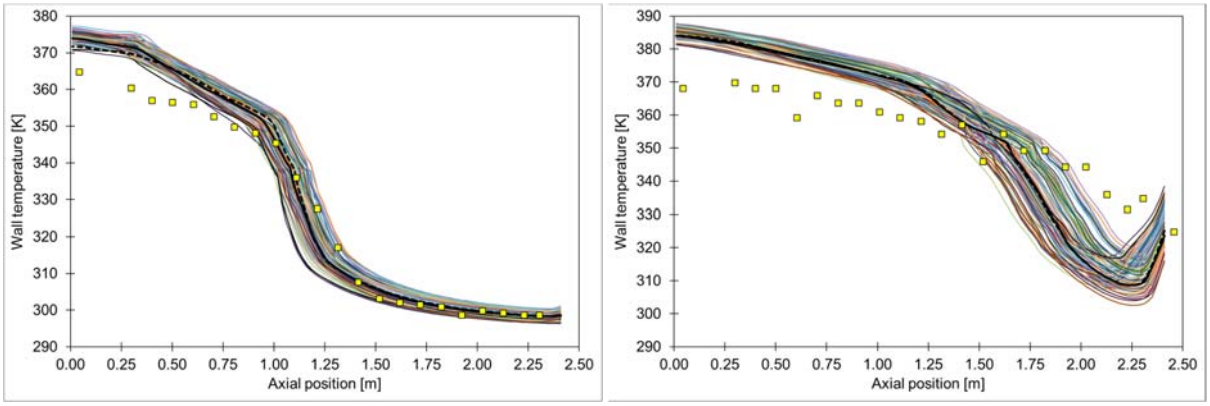


**Figure 5. Wall temperatures of the experiments (symbols) compared to calculated temperatures (lines). Bold line indicates reference calculations, broken lines indicate average values based on the 93 simulations. Case 163 – left, case 175 – right.**

Nevertheless, the uncertainty and sensitivity study can be used to identify the most important input and boundary conditions for this particular condensation experiment. This information might be relevant during the modelling of condensation phenomena with TRACE in general and in particular for the tuning of these parameters. The plots in Figure 6 show the partial correlation coefficient (P.C.C.) for the Pearson's product momentum correlation (definitions can be found in [18] [19]) with respect to the wall temperature, given in Figure 5. This coefficient is a measure for the linear relation of one parameter to the result(s), after eliminating the linear effects of other parameters on the result(s). Thereby, the numerical value indicates the strength of the linear relation (0 = no relation; 1 = perfect relation), while the algebraic sign indicates the proportionality. A "+" sign indicates a direct proportional relation, while a "-" indicates inversely proportional relations. Only the most sensitive parameters are shown for the sake of readability. Taking the left plot of Figure 6 (case 163) as example, the most interesting observation is that for most parameters no clear distinction can be made between the zone with actual steam condensation (0.0 m … 1.0 m) and the zone with liquid water forced convection (1.5 m …2.5 m). Parameters 1, 2 and 4 (vapour and coolant mass flow rate, coolant temperature) show high P.C.C. values over almost the whole axial length. The transition from pure steam condensation to two-phase flow at around 1.3 m is visible just by small depressions in the trends of parameters 1, 2 and 4. Below 0.5 m some larger fluctuations are visible. The only parameter with larger fluctuations along the total length is the parameter 6, the wall roughness.

The wall roughness is connected to the condensing heat transfer by the heat transfer model of Gnielinski, which uses the friction factor. In addition, the wall roughness influences the calculation of the pressure and subsequent the calculation of the corresponding saturation temperature. Interesting to observe is also that the vapour inlet temperature is of almost no importance. Below 1.0 m it can be neglected, while at around 2 m only a small relation and dependency is visible between the steam temperature and the wall temperature. An explanation could be that the initial steam inlet temperature is more than 10 K above the saturation temperature at the corresponding initial pressure, see Table I. Hence, the superheated state of the steam will be maintained even for small variations of the steam temperature. The main difference between cases 163 and 175 with respect to the P.C.C. is the importance of parameter 6, the wall roughness. For case 163, an up-and-down trend is visible over the total length, while for case 175 a sharp transition from direct to inverse proportionality is present on the first 0.75 m. For the remaining length, an inversely proportional relationship (increasing wall temperature following a decreasing wall roughness) prevails.

With respect to the main intention of the present paper, the identification of the varying success in the post-test calculation of steam condensation experiments, it can be stated that the uncertainty and sensitivity study did not reveal a satisfying reason for the differences.

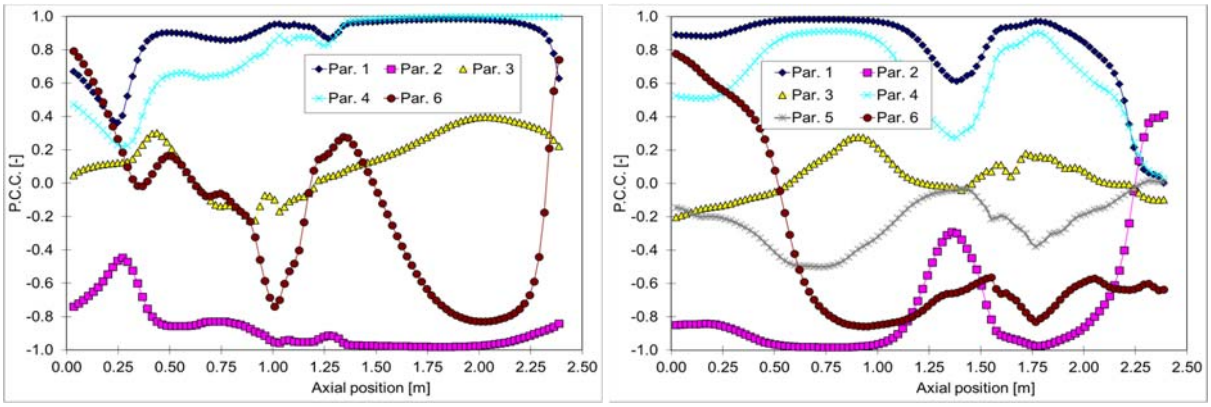


**Figure 6. P.C.C. for Pearson's product momentum coefficient. Case 163 – left, case 175 – right.**

## 5. EVALUATION OF EMPIRICAL CONDENSATION MODELS

The condensation models introduced in section 2 are implemented into the TRACE source code. For each new TRACE version, the two selected experimental cases (163 and 175) are executed. The results for the calculated wall temperatures are plotted in figure Figure 7. The comparison shows that the qualitative trend is identical for all condensation models in both cases. Only (small) qualitative changes are visible. From the left plot of Figure 7 it can also be concluded, that the standard model gives the best representation of the experimental scenarios. This statement holds also for the other successful cases, which are not shown in this paper due to page limitations. With respect to case 175, as a representative for the unsuccessful simulation, it cannot be determined if one condensation model is better than the others. In principle, this outcome is not expected, because the different condensation models produce Nusselt numbers (heat transfer coefficients) considerably different. To illustrate that, the heat flux and the corresponding heat transfer coefficients are plotted in Figure 8 and Figure 9, respectively. For both cases, the values for the calculated heat flux do not differ significantly. The differences are in the range of up to +25 % at around 0.85 m for case 163. However, the heat transfer coefficient varies by up to a factor of 4 between the different models at the same axial position. The reason for the large deviation in heat transfer coefficient may be found in the definition of the heat transfer coefficient.

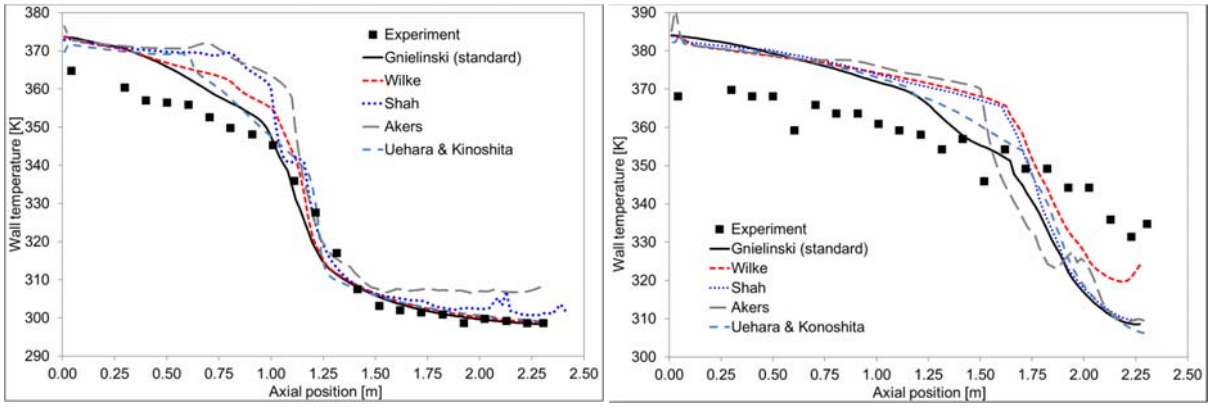


**Figure 7. Calculated wall temperature based on different condensation models. Case 163 – left, case 175 – right.**

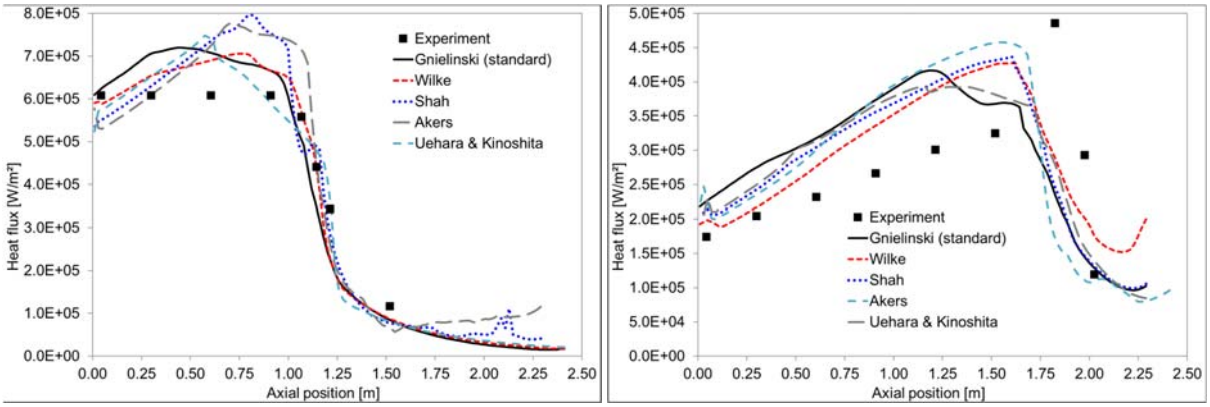


**Figure 8. Calculated heat flux based on different condensation models. Case 163 – left, case 175 – right.**

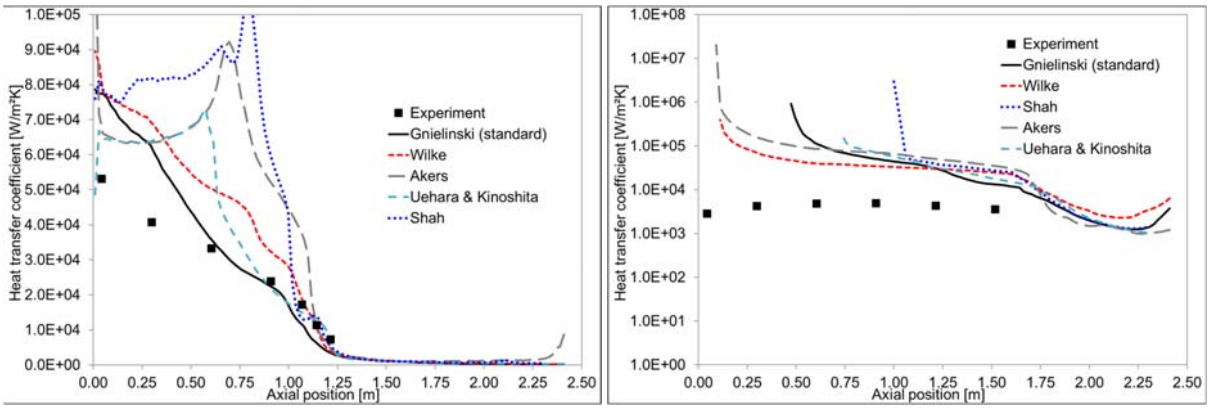


**Figure 9. Calculated heat transfer coefficient based on different condensation models. Case 163 – left, case 175 – right.**

In the experiment, the local condensing heat transfer coefficient is defined as follows:

$$h_{\text{condensing}} = \frac{q_{\text{inner surface}}}{(T_{\text{saturation}} - T_{\text{wall}})}. \tag{22}$$

Depending on the difference between the wall temperature and the local saturation temperature, a rather large heat transfer coefficient is calculated. Especially for small temperature differences, large heat transfer coefficients are calculated. For case 163 the difference is in the range of 26 K (at 0.8 m) with the standard Gnielinski model and 7 K with the Shah model. Hence, large discrepancies occur. With respect to case 175, in general, a qualitative agreement is given for the heat flux calculation of 175, but not for the wall temperature. It looks like that the experimental wall temperature does not correspond to the experimental heat flux. The wall temperature steadily decreases with the length, while for the heat flux a smooth increase is followed by a sharp decrease (at 1.75 m, see right plot of Figure 8). This different behaviour is not found for case 163, where the trend of the wall temperature is consistent with the heat flux. Furthermore, the calculation of the heat transfer coefficient according to Eq. (22) leads to negative values during the calculations, because at some point the wall temperature exceeds the saturation temperature. Hence, for case 175, steam entering the condenser is condensed and re-evaporated further downstream. It is not clear to the authors if that behaviour is physical sound or if it is a numerical issue related to the condensing models. Together with the non-corresponding experimental data for wall temperature, heat flux and heat transfer coefficient, flaws in the experiment as well as in the calculations might be present for case 175.

## 6. SUMMARY AND DISCUSSION

In the present contribution, a high-velocity steam condensation experiment is modelled with TRACE. Due to previous investigations, leading to unsatisfying results in terms of reproducibility of some experimental cases, a more comprehensive modelling approach is pursued. Thereby, selected experimental scenarios, one which can be reproduced with TRACE and one which cannot, are selected for an uncertainty and sensitivity study. This study shows, first, that variations of the input and boundary conditions did not cause a qualitative change in the trend for selected output parameters (wall temperature as function of the axial length). Second, the main parameters influencing the quantitative changes of the output are the mass flow rates of the steam and the coolant, as well as the coolant inlet temperature. A higher steam inlet mass flow rate results in higher wall temperatures, while a higher coolant inlet mass flow rate reduces the wall temperature. Furthermore, an increase of the coolant inlet temperature leads to an increase of the wall temperature. Interesting to see is the influence of the wall roughness on the wall temperature. Due to the

strong changes of proportionality along the axial length, it cannot be stated how important this parameter is. It might be possible that this parameter loses its importance as soon as other condensation models are used, because the standard TRACE model uses the friction factor as an input for the Nusselt number.

In addition to the uncertainty and sensitivity study, an assessment of different condensation models is performed. Four different models are taken from the literature and are implemented into the TRACE source code. The two previously selected experimental scenarios are simulated with each new TRACE version. The comparison to the experimental data and the standard TRACE condensation model shows no significant qualitative changes of selected parameters like wall temperature and heat flux. In principle, the current condensation model of TRACE, the Gnielinski model, performs very well for most of the cases. The experimental cases not accessible with the standard model are not accessible with new condensation models either.

The major outcome of this study is that some experimental scenarios of an experimental campaign for high-velocity steam condensation cannot be modelled with the system code TRACE. Neither an uncertainty and sensitivity study nor an assessment and application of different condensation models helped to calculate figures, which are in agreement or even comparable to the experimental data. One reason might be, that the experimental data are flawed. Either the measurements are wrong or the measurements do not correspond to the corresponding input and boundary condition. It is shown, that the wall temperatures and the heat flux of case 175 do not correspond to each other, as one would expect. The authors are aware that claiming an experiment might be wrong, because the calculations do not fit to it, is a severe and bold statement. Based on own experience, the authors know that flaws happen in the experiment itself as well as in its documentation. The next step in the process of post-test calculations of the introduced experiment is the definition of a benchmark, which includes other codes as well as other code users. Currently, the efforts aim to include RELAP, MELCOR and ASTEC, all of them are available at the institutions of the authors. Other institutions and codes are welcome.

**NOMENCLATURE**

| | |
|---|---|
| $c_p$ | Specific heat capacity |
| $f$ | Friction factor |
| $G$ | Film mass flux |
| $g$ | Acceleration of mass |
| $h$ | Heat transfer coefficient |
| $k$ | Thermal conductivity |
| $p$ | Pressure |
| $q$ | Heat flux |
| $T$ | Temperature |
| $x$ | Vapour quality |
| $\delta$ | Film thickness |
| $\eta$ | Dynamic viscosity |
| $\nu$ | Kinematic viscosity |
| $\rho$ | Density |
| $\sigma$ | Surface tension |
| Gr | Grashof number |
| Ja | Jakob number |
| Nu | Nusselt number |
| Pr | Prandtl number |
| Re | Reynolds number |
| So | Soflata number |

## REFERENCES


1. W. Jaeger, W. Hering, “Post-test analysis of a high-velocity steam condensation experiment with the system code TRACE,” *Proceedings of the 17th International Topical Meeting on Nuclear Reactor Thermal Hydraulics*, Xi’an, China, September 3-8 (2017).
2. J.H. Goodykoontz and R.G. Dorsch, “Local heat-transfer coefficients and static pressures for condensation of high-velocity steam within as tube,” NASA Technical Note NASA TN D-3953 (1967).
3. U.S. NRC, "TRACE V5.0 Theory manual," US NRC, Washington, D.C. (2012).
4. S.Z. Kuhn, V.E. Schrock and P.F. Peterson, "Final Report on U. C. Berkeley Single Tube Condensation Studies," UCB-NE-4201 (1994).
5. S.Z. Kuhn, V.E. Schrock and P.F. Peterson, Interfacial shear and waviness effects on laminar film flow heat transfer in vertical tubes,” *Proceedings of the 31st National Heat Transfer Conference*, Houston, Texas, USA, August 3-6 (1996).
6. V. Gnielinski, "New Equations flow regime Heat and Mass Transfer in Turbulent Pipe and Channel Flow," *International Chemical Engineering*, **16**, pp. 359-368 (1976).
7. G.K. Filonenko, "Hydraulic Resistance in Pipes," (in Russian), *Teplonergetika*, **1**, pp. 40-44 (1954).
8. W. Wilke, “Waermeuebergang an Rieselfilmen (in German),” VDI-Forschungsheft 490, Vol. B, No. 28, 1962.
9. M.M. Shah, “A general correlation for heat transfer during film condensation inside pipes,“ *Int. J. Heat Mass Transfer*, **22**, pp. 547-556 (1979).
10. Karls Stephan, “*Heat transfer in condensation and boiling*,“ Springer, Berlin, Germany (1992).
11. W.W. Akers, H.A. Deans, O.K. Crosser, “Condensing heat transfer within horizontals tubes,” *Chem. Eng. Progr. Symposium Ser.* **55(**29), pp. 171-176 (1959).
12. H. Uehara, E. Kinoshita, “Wave and turbulent film condensation on a vertical surface (correlation for local heat-transfer coefficient),” *Trans. Jpn. Soc. Mech. Eng*., **60**, pp. 3109-3116 (1994).
13. H. Uehara, E. Kinoshita, “Wave and turbulent film condensation on a vertical surface (correlation for average heat-transfer coefficient),” *Trans. Jpn. Soc. Mech. Eng.*, **63**, pp. 4013-4020 (1997).
14. S.G. Kandlikar, M. Shoji, V.K. Dhir, “*Handbook of phase change: Boiling and condensation*,” Taylor & Francis, Philadelphia, PA, U.S.A. (1999).
15. H. Glaeser, “GRS method for uncertainty and sensitivity evaluation of code results and application,” *Sci. Technol. Nucl. Install*., ID 798901 (2008).
16. B. Krzykacs, E. Hofer, M. Kloos, “A software system for probabilistic uncertainty and sensitivity analysis of results from computer models*,” Proceedings of the International Conference on Probabilistic Safety Assessment and Management*, San Diego, CA, USA, March 20-25 (1994).
17. S. Wilks, “Determination of sample size for setting tolerance limits,” *Ann. Math. Stat*., **13**, pp. 91-96 (1941).
18. W.J. Conover, “*Practical Nonparametric Statistics*,“ 2nd Ed., Wiley Ed., New York, U.S.A. (1980).
19. W. Jaeger, V.H. Sánchez Espinoza, “Uncertainty and sensitivity study in the frame of TRACE validation for reflood experiments”, *Nuclear Technology*, **183**, pp. 333-350 (2013).